Enhancement of Power Flow with Reduction of Power Loss Through Proper Placement of FACTS Devices Based on Voltage Stability Index

Yeshitela Shiferaw(✉) and K. Padma

College of Engineering (A), Andhra University, Visakhapatnam 530003, Andhra Pradesh, India
Yeshitela2010@gmail.com, padma315@gmail.com

Abstract. One of the significant problems in the power system network is the overloading of the transmission system which increases stress on transmission lines. This problem can be mitigated by the addition of isolated and individually controlled devices such as FACTS to the existing networks. Thus, the main objective of this paper is determining the optimal placement of SVC and TCSC FACTS device at bus and lines and minimizing the total power loss & enhances the transferred power by applying these SVC and TCSC FACTS devices. To this end, first, load flow analysis was done using the Newton Raphson technique. Then, the optimal location was found by the voltage stability index (L-indices) and fast voltages stability indices (FVSI). The critical bus has the lowest voltage and the critical line has the largest value of FVSI. Consequently, SVC and TCSC FACTS device is installed on both the critical bus and the critical line respectively. To validate the methodology, we use IEEE-30 bus standard test system network and the simulation is done on PSAT (power system analysis toolbox) in MATLAB. Finally, based on the finding of the simulation result, the best locations for SVC and TCSC FACTS devices for improving power transfer, voltage profile and loadability are the weakest bus and line of the system.

Keywords: Optimal placement · Thyristor control series compensator · Static var compensator · Loadability · Voltage stability index

1 Introduction

The major problem of a heavily loaded system is that the transmission network operates near to its limit. This, in turn, leads to the increment of stress on the transmission. This problem was solved by the addition of isolated and individually controlled devices such as FACTS to the existing networks.

The power flow analysis is necessary for power system planning, new power generation, new transmission line and load scheduling. It is crucial in placing FACT devices in the weak bus and weak lines. FACTS devices can be fully utilised if the optimal location is determined through specific techniques. Here, the voltage stability index calculation method was used for the optimal position of the TCSC and SVC FACTS devices [1].

N. G. Habtu et al. (Eds.): ICAST 2019, LNICST 308, pp. 355–365, 2020.
https://doi.org/10.1007/978-3-030-43690-2_24

The purpose of this study is to illustrate the applications of voltage stability indexes. In line with these indexes were found to be effective in detecting the weakest bus and line in the system. Moreover, the addition of SVC and TCSC FACTS devices on the weakest bus and line has improved the voltage profile, total power loss and loadability of the system. Standard IEEE-30 bus test system network and MATLAB/PSAT were used to validate the methodology.

Criteria for selection of optimal locations.

During steady-state operation, FACTS devices can be considered as a Controllable reactance connected in series with the line and with the bus. The effects of the insertion of FACTS devices [2, 3]:

- Reduces transfer reactance between the two buses.
- Increases transfer capability of the line.
- Reduces reactive power loss.
- Improves the voltage profiles.

The criteria for the optimal placement of FACTS devices are as follows [3, 4, 5]:

- The device should be placed in a line which has the least sensitivity concerning the magnitude of static reactance.
- The sending end bus must be either a load bus or a generator bus with no regulating generation.
- The device should be placed in a line which has the most substantial absolute value of the sensitivity concerning the phase angle.
- The device should not be placed in the line containing generation buses even if the sensitivity is the highest.
- The terminal end bus should not have a switched shunt connected to it.
- Multiple devices sending end on the same bus can be allowed.

2 Voltage Stability Analysis Using Bus and Line Index

The main goal of voltage stability indices is to determine voltage instability within the system network [6, 7]. These indices are referred either to a bus or a line.

2.1 Voltage Stability Index (L-Index)

The load flow algorithms incorporate load and generator control characteristics. The voltage stability indices value is changed between zero (no load) and one (voltage collapse) based on the solution of load flow using Newtown Raphson, the L index [8] can be calculated as:

$$L_j = \left| 1 - \sum_{i=1}^{ng} F_{ji} \frac{V_i}{V_j} \right| \tag{1}$$

Where $ng \in [0, n]$. F_{ji} is attained from the Y bus matrix as follows:

$$\begin{pmatrix} I_G \\ I_L \end{pmatrix} = \begin{pmatrix} Y_{GG} & Y_{GL} \\ Y_{LG} & Y_{LL} \end{pmatrix} \begin{pmatrix} V_G \\ V_L \end{pmatrix} \tag{2}$$

Where I_G, I_L, V_G, V_L, represents current and voltages at the generator and load buses.

Rearranging (2), it can be written as

$$\begin{pmatrix} V_L \\ I_G \end{pmatrix} = \begin{pmatrix} Z_{LL} & F_{LG} \\ Y_{GL} & Y_{GG} \end{pmatrix} \begin{pmatrix} I_L \\ V_G \end{pmatrix} \tag{3}$$

Where $F_{LG} = -[Y_{LL}]^{-1}[Y_{LG}]$ are the necessary values, the L indices for a given load condition are computed for all load buses.

The equation for the L index for the node can be written as

$$L_j = \left| 1 - \sum_{i=1}^{ng} F_{ji} \frac{V_i}{V_j} \angle \theta_{ij} + \delta_i - \delta_j \right| \tag{4}$$

Where θ_{ij} is the power factor angle and δ_i & δ_j are voltage angle of the i^{th} and j^{th} bus respectively.

Algorithm to obtaining voltage stability indices are [6, 9].

Step one: form admittance matrix (Y-bus) for the system
Step two: find the element of F_{LG} from Eq. (3)
Step three: find the value of L-indices using Eq. (4) by applying step two

2.2 Line Stability Index (Fast Voltage Stability Index)

The line stability index (fast voltage stability index) projected by Musirin *et al.* [10] is based on a conception of power flow through a single transmission line. For a significant transmission line, the fast voltage stability index is defined by:

$$FVSI_{ij} = \frac{4Z^2 Q_j}{V_i^2 X_{ij}} \tag{5}$$

Where Z = line impedance, X_{ij} = line reactance, Q_j = reactive power at the receiving end and V_i = sending end voltage.

The line voltage stability indices which show that FVSI is very close to unity (1.0) implies that it is approaching the point of instability. If FVSI is starting to be higher than unity, this is the indication of voltage collapse in the system network due to a sudden drop in voltage [11].

3 SVC Thyristor Modeling (B = Bscv)

The SVC can be variable reactance by using firing-angle limits or reactance limits, as it is shown in Fig. 1. The SVC nonlinear power equation is derived from variable shunt compensator modelling and changed to the linear equation by Newton's method.

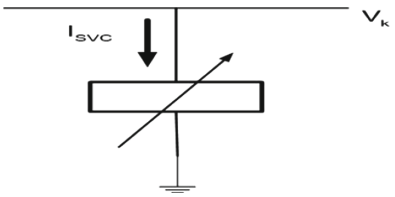

Fig. 1. Variable shunt susceptance

From Fig. 1 the current drawn by SVC and reactive power injected at bus K is

$$I_{SVC} = jB_{SVC} * V_K \tag{6}$$

$$Q_{SVC} = Q_K = -V_k^2 * B_{SVC} \tag{7}$$

The linearised equation is given by Eq. (7) where the equivalent susceptance B_{SVC} is taken to be the state variable

$$\begin{bmatrix} \Delta P_K \\ \Delta Q_K \end{bmatrix}^i = \begin{bmatrix} 0 & 0 \\ 0 & Q_K \end{bmatrix}^i \begin{bmatrix} \Delta\theta_K \\ \Delta B_{SVC}/B_{SVC} \end{bmatrix}^i \tag{8}$$

The variable shunt susceptance B_{SVC} is updated at the end of the iteration (i) is

$$B_{SVC}^i = B_{SVC}^{(i-1)} + \left(\frac{\Delta B_{SVC}}{B_{SVC}}\right)^{(i)} B_{SVC}^{(i-1)} \tag{9}$$

This changing susceptance characterises the total SVC susceptance essential to keep the nodal voltage magnitude at the specific value. Once the level of compensation has been determined, the firing angle required to achieve such compensation level can be calculated.

4 TCSC Variable Series Impedance Modeling

The variable series compensation is hugely effective in both controlling power flow in the line and in improving the stability of the power system within the ranges of the system [12, 13].

The amount of reactance is determined efficiently using Newton's method.

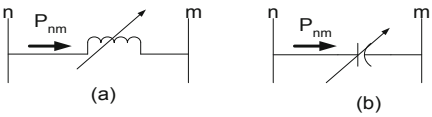

Fig. 2. TCSC equivalence circuit: (a) inductive and (b) capacitive type.

The transfer admittance matrix of the variable compensator shown in the Fig. 2 is

$$\begin{bmatrix} I_n \\ I_m \end{bmatrix} = \begin{bmatrix} jB_{nn} & jB_{nm} \\ jB_{mn} & jB_{mm} \end{bmatrix} \begin{bmatrix} V_n \\ V_m \end{bmatrix} \tag{10}$$

The active and reactive power equations at bus n are:

$$P_n = V_n V_m B_{nm} \sin(\theta_n - \theta_m) \tag{11}$$

$$Q_k = -V_k^2 B_{nn} - V_n V_m B_{nm} \cos(\theta_n - \theta_m) \tag{12}$$

The set of linearised power flow equations are:

$$\begin{bmatrix} \Delta P_n \\ \Delta P_m \\ \Delta Q_n \\ \Delta Q_m \\ \Delta P_{nm}^{XTCSC} \end{bmatrix} = \begin{bmatrix} \frac{\partial P_n}{\partial \theta_n} & \frac{\partial P_n}{\partial \theta_m} & \frac{\partial P_n}{\partial V_n} V_n & \frac{\partial P_n}{\partial V_m} V_m & \frac{\partial P_n}{\partial X_{TCSC}} X_{TCSC} \\ \frac{\partial P_m}{\partial \theta_n} & \frac{\partial P_m}{\partial \theta_m} & \frac{\partial P_m}{\partial V_n} V_n & \frac{\partial P_m}{\partial V_m} V_m & \frac{\partial P_m}{\partial X_{TCSC}} X_{TCSC} \\ \frac{\partial Q_n}{\partial \theta_n} & \frac{\partial Q_n}{\partial \theta_m} & \frac{\partial Q_n}{\partial \theta_n} V_n & \frac{\partial Q_n}{\partial \theta_m} V_m & \frac{\partial Q_n}{\partial X_{TCSC}} X_{TCSC} \\ \frac{\partial Q_m}{\partial \theta_n} & \frac{\partial Q_m}{\partial \theta_m} & \frac{\partial Q_m}{\partial \theta_n} V_n & \frac{\partial Q_m}{\partial \theta_m} V_m & \frac{\partial Q_m}{\partial X_{TCSC}} X_{TCSC} \\ \frac{\partial P_{nm}^{X_{TCSC}}}{\partial \theta_n} & \frac{\partial P_{nm}^{X_{TCSC}}}{\partial \theta_m} & \frac{\partial P_{nm}^{X_{TCSC}}}{\partial \theta_n} V_n & \frac{\partial P_{nm}^{X_{TCSC}}}{\partial \theta_m} V_m & \frac{\partial P_{nm}^{X_{TCSC}}}{\partial X_{TCSC}} X_{TCSC} \end{bmatrix} \begin{bmatrix} \Delta\theta_n \\ \Delta\theta_m \\ \frac{\Delta V_n}{V_n} \\ \frac{\Delta V_m}{V_m} \\ \frac{\Delta X_{TCSC}}{X_{TCSC}} \end{bmatrix} \tag{13}$$

Where $\partial P_{nm}^{X_{TCSC}}$ is the active power flow mismatch for the series reactance calculate as follow

$\partial P_{nm}^{X_{TCSC}} = P_{nm}^{reg} - P_{nm}^{X_{TCSC,cal}}$, and ΔX_{TCSC} is given by $\Delta X_{TCSC} = X_{TCSC}^{(i)} - X_{TCSC}^{(i-1)}$

The state variable XTCSC of the series controller is updated at the end of each iterative step according to

$$X_{TCSC}^{(i)} = X_{TCSC}^{(i-1)} + \left(\frac{\Delta X_{TCSC}}{X_{TCSC}} \right)^i X_{TCSC}^{(i-1)} \tag{14}$$

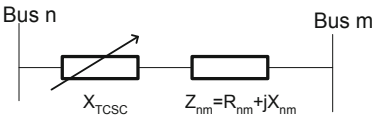

Fig. 3. Modelling of transmission line with TCSC

The model of transmission line with a TCSC connected between bus *n* and bus m is shown in Fig. 3

$$X_{line} = X_{nm} + X_{TCSC} \tag{15}$$

Where X_{nm} is the reactance of the line between bus n and m without TCSC reactance, and the reactance X_{TCSC} is restricted to the domain.

$X_{TCSC,\min} \leq X_{TCSC} \leq X_{TCSC,\max}$ Where the values of X_{TCSC}, *min* and X_{TCSC}, *max* are determined by the size of the TCSC device and the characteristics of the line in which it is placed.

5 Continuous Power Flow

A conventional power flow has a problem during a Jacobian matrix which becomes singular at the voltage stability limit; this problem can be overcome by using continuous power flow [13]. The graph obtained using continuous power flow methods between bus voltage, and the loading factor λ is a P-V curve. It determines the loadability of margins. The flow chart describes in Fig. 4 shows the steps to solve continuous power flow analysis.

5.1 Mathematical Reformulations

Reformulating Newton Raphson load flow Equations to include loading factor λ.

The conventional Newton Raphson load flow equations can be as follow

$$P_i = V_i \sum_{j=1}^{n} V_j Y_{ij} \cos(\theta_i - \theta_j - \delta_{ij}) \tag{16}$$

$$Q_i = V_i \sum_{j=1}^{n} V_j Y_{ij} \sin(\theta_i - \theta_j - \delta_{ij}) \tag{17}$$

Conventional power flow equations modified by incorporating of λ

$$P_{Li} = P_{Li0}(1 + \lambda K_{Li}) \tag{18}$$

$$Q_{Li} = Q_{Li0}(1 + \lambda K_{Li}) \tag{19}$$

$$P_{Gi} = P_{Gi0}(1 + \lambda K_{Gi}) \tag{20}$$

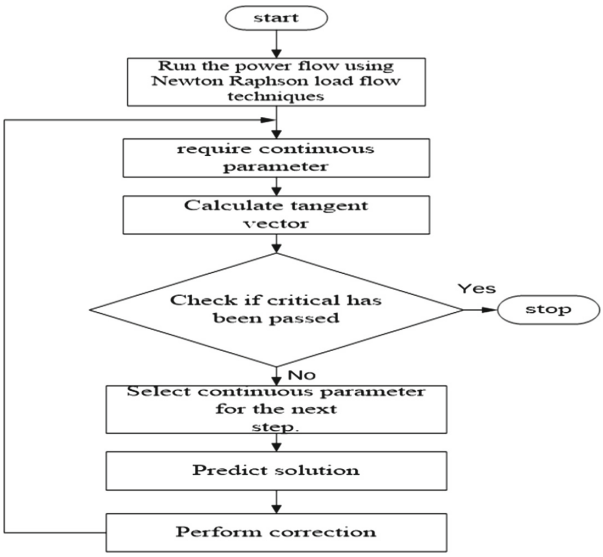

Fig. 4. Flow chart of the continuous power flow [13]

Applying continuous power flow algorithm to these equations, and the whole set of equations can be written as:

$$F(\theta, V, \lambda) = 0 \tag{21}$$

Predict, and corrector steps can be given by the following Eqs. (22) and (23) respectively.

$$\begin{bmatrix} F_\theta & F_V & F_\lambda \end{bmatrix} \begin{bmatrix} d\theta \\ dV \\ d\lambda \end{bmatrix} = 0 \tag{22}$$

$$\begin{bmatrix} F(x) \\ x_k - \eta \end{bmatrix} = 0 \tag{23}$$

6 Result and Discussion

The system simulation and load flow equations are solved; voltage stability indices (L-indices) and fast voltage stability indices (FVSI) are simulated to determine the weakest bus and line in the system. The results of the comparison and the performance of the system with and without FACTS devices are presented in this section.

IEEE 30 bus system network consists of six generating units interconnected with 41 branches of a transmission network with a total load of 283.4 MW and 126.2 MVAR, four transformers with off-nominal tap ratio, as its shown in Fig. 5. The bus data and the branch data are taken from [14].

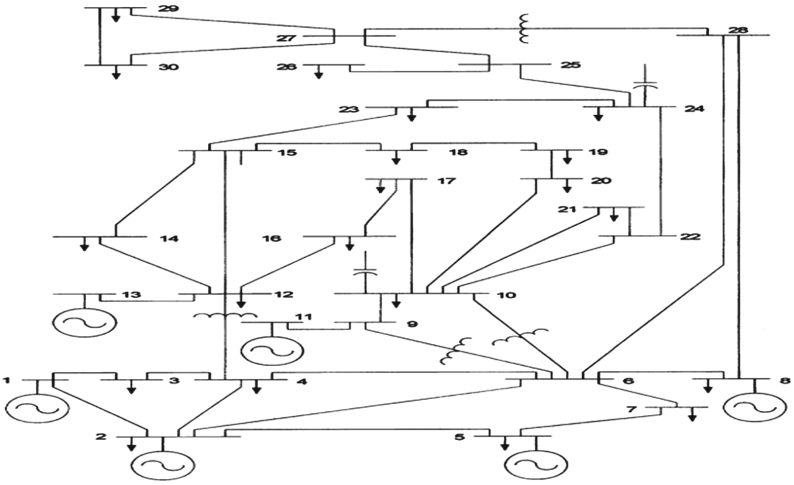

Fig. 5. IEEE-30 bus standard test system diagram [14]

For incorporating power flow with FACTS devices, power system analysis toolbox (PSAT) is used in MATLAB software. This power system analysis toolbox is helpful for power system analysis and control including optimal power flow as well as continuous power flow analysis [5].

6.1 P-V Curve

Before analysing P-V curves, we have to find out the weakest bus and line using voltage stability index computation. From Table 1, it is observed that the five most critical bus and lines are selected. Besides, as it can be seen from Fig. 6, bus number 26 exhibits the highest voltage stability index which means it is the weakest bus in the system. From Table 1, it is noted that the line which connects between bus 3 and 4 is the most critical based on the stability indices of lines. Voltage collapse can be accurately predicted when the index is more than one. The line that gives index value closest to one should be the most critical line of the bus and may lead to the instability of the whole system.

Table 1. Voltage stability index

Line stability index			Bus stability L-index	
From bus	To bus	Voltage stability index (FVSI)	Bus no	L-index
3	4	0.20585	26	0.0761
2	6	0.11878	30	0.0729
2	4	0.09494	24	0.0715
4	12	0.09014	19	0.0715
1	3	0.08590	18	0.0697

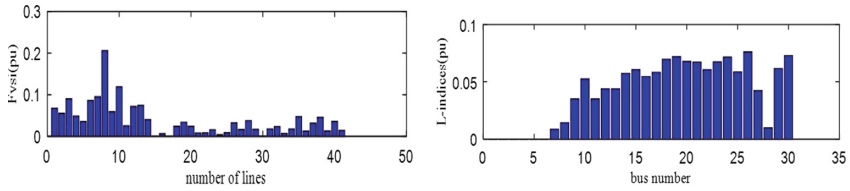

a) Fast voltage stability indices (FVSI) b) Bus stability indices (L-indices)

Fig. 6. Voltage stability index

The variations of bus voltage with the loading factor λ were obtained for IEEE-30 bus system network. The loading factor was one at the base case and gradually increased until the loading point reached the maximum. It was found that bus number 26 was the most insecure bus as the voltage at each reactive load of bus 26 was minimum. Figure 7(a) shows the P-V curve for the lowest five voltage buses without SVC, and the loading parameter is 3.4362 pu. Figure 7(b) shows the P-V curve for five most economical voltage buses with SVC at bus 26, and the loadability setting (λ) increased to 3.447 pu. It clearly showed that the load ability margin had risen significantly.

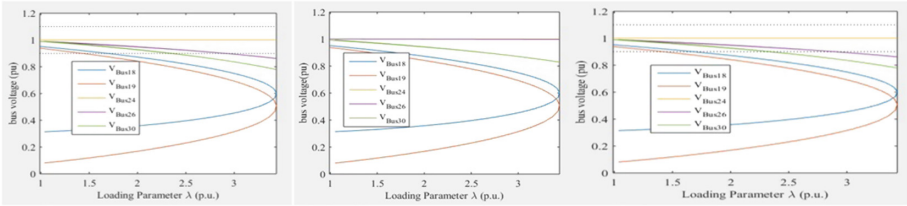

a) P-V curves without SVC FACT device. b) P-V curves when SVC connected at bus 26. c) P-V curves when TCSC connected between bus 3 and 4

Fig. 7. P-V curve without and with SVC FACTS device

6.2 Performance of the System with TCSC and SVC Facts Devices

The consolidated comparative bus voltage results have been represented in Fig. 8(a). The use of SVC shunt compensator has improved network voltage profile and keeps the voltage magnitude at 1 p.u at bus 26. The real power flow for thirty bus system was analysed without and with FACTS device in Fig. 8(b) from the result the TCSC series compensator model is to maintain the active power flow between bus 3 and 4 as compared to SVC shunt compensator. Similarly, in Fig. 8(c) the TCSC series compensator was more applicable to reduce the real power loss in the line.

As clearly shown in Table 2. The instalment of SVC is not only improving the system voltage profile but also reduces total real power losses. The actual power loss after installing SVC at bus 26 is reduced by 0.124%. Similarly, TCSC FACTS device reduce total power loss by 2.813%. While as result TCSC FACTS device is more significant for total real power loss.

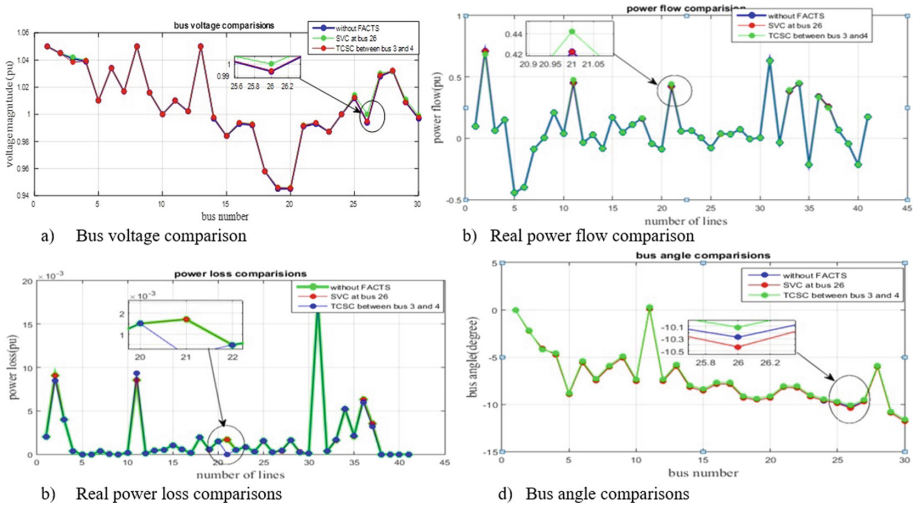

Fig. 8. Performance of TCSC and SVC FACTS devices comparison

Table 2. Total power loss comparison with and without SVC and TCSCFACTS device

No	Power loss (pu) without FACTS devices	Power loss (pu), SVC @bus 26	Power loss (pu), TCSC b/n 3 and 4 bus
	0.075576	0.075482	0.07345
Reduced by		0.124%	2.813%

7 Conclusion

The paper analyzed voltage stability indices for selecting the weak bus and line and put the SVC and TCSC FACTS device on this weak bus and line for the improvement of bus voltage and power flow on the line. Here are the main contributions.

- Weak bus and line are identified using voltage stability indexes
- The voltage profile for all the buses was obtained.
- Power transfer in each line was attained.
- Loadability was compared with and without SVC FACTS device.
- TCSC FACTS device which was connected between bus-3 and bus-4 showed great improvement in reducing total real and reactive power loss.
- SVC FACTS device which was connected on bus-26 has improved real power loss and loadability.
- The use of FACTS device in both at bus and line reduces power loss and improves system voltage profile

Acknowledgements. We would like to acknowledge the support of Defense University, Engineering College, research and development Centre, Ethiopia and Andhra University, Electrical Engineering Department, India.

References

1. Liu, Q., You, M., Sun, H., Matthews, P.: L-index sensitivity based voltage stability. School of Engineering and Computing Sciences, Durham, UK (2017)
2. Kazemia, B.B.A.: Modeling and simulation of SVC and TCSC to study. Electr. Power Energy Syst. **26**, 381–388 (2004)
3. Padhy, N.P., Abdel-Moamen, M.A.: Optimal placement of FACTS devices for practical utilities. Int. J. Power Energy Syst. **27**(2), 193–204 (2007)
4. Vanfretti, L., Milano, F.: The experience of PSAT (power system analysis toolbox) as a free and open source software for power system education and research. Int. J. Electr. Eng. **25**(12), 1–28 (2008)
5. Milano, F.: An open source power system analysis toolbox. IEEE **25**(2), 1–8 (2004)
6. Chengaiah, Ch., Satyanarayana, R.V.S., Mrutheswar, G.V.: Location of UPFC in electrical transmission system: fuzzy contingency ranking and optimal power flow. Int. J. Eng. Res. Dev. **1**(12), 10–20 (2012)
7. Kumar, S., Kumar, A., Sharma, N.K.: A novel method to investigate voltage stability of IEEE-14 bus wind integrated system using PSAT. Front. Energy (6), 2–8 (2016). https://doi.org/10.1007/s11708-016-0440-8
8. Reddy, V.R.K., Lalitha, M.P.: Identification of instability and its enhancement through the optimal placement of facts using L-index method. J. Theor. Appl. Inf. Technol. **60**(3), 616–622 (2014)
9. Chakrabarti, A.: Electricity Pricing Regulated, Deregulated and Smart Grid Systems. Taylor & Francis Group, Kolkata (2014)
10. Musirin, I.: Novel fast voltage stability index (FVSI) for voltage stability analysis. In: Research and Development Proceedings, Shah Alam Malaysia (2002)
11. Ambriz-Perez, H., Acha, E.: Advanced SVC models for Newton-Raphson load flow and Newton optimal power flow studies. IEEE Trans. Power Syst. **15**(1), 129–131 (2000)
12. Lakshan Piyasinghe, Z.M.: Impedance-model-based SSR analysis for type 3 wind generator and series-compensated network. IEEE Trans. Sustain. Energy **5**(1), 179–187 (2015)
13. Ajjarapu, V.: The continuation power flow: a tool for steady state voltage stability analysis. IEEE Trans. Power Syst. **7**(1), 416–423 (1992)
14. Üney, M.Ş.: Optimal power flow and load flow analysis with considering different DG integration rates. Asian J. Appl. Sci. Technol. (AJAST) **1**(9), 542–549 (2017)